Original article

Static and dynamic behavior of steel-reinforced epoxy granite CNC lathe bed using finite element analysis

Shanmugam Chinnuraj[1] ![ORCID], PR Thyla[1], S Elango[2],
Prabhu Raja Venugopal[1], PV Mohanram[3],
Mahendrakumar Nataraj[1], S Mohanraj[1], KN Manojkumar[1]
and Siddarth Ayyasamy[1]

Abstract

Machine tools are used to manufacture components with desired size, shape, and surface finish. The accuracy of machining is influenced by stiffness, structural damping, and long-term dimensional stability of the machine tool structures. Components machined using such machines exhibit more dimensional variations because of the excessive vibration during machining at higher speeds. Compared to conventional materials like cast iron, stone-based polymer composites such as epoxy granite have been found to provide improved damping characteristics, by seven to ten folds, due to which they are being considered for machine tool structures as alternate materials. The stiffness of structures made of epoxy granite can be enhanced by reinforcing with structural steel. The current work highlights the design and analysis of different steel reinforcements in the lathe bed made of the epoxy granite composite to achieve equivalent stiffness to that of cast iron bed for improved static and dynamic performances of the CNC lathe. A finite element model of the existing the cast iron bed was developed to evaluate the static (torsional rigidity) and dynamic characteristics (natural frequency) and the results were validated using the experimental results. Then finite element models of five different steel reinforcement designs of the epoxy granite bed were developed, and their static and dynamic behaviors were compared with the cast iron bed through numerical simulation using finite element analysis. The proposed design (Design-5) of the epoxy granite bed is found to have an improvement in dynamic characteristics by 4–10% with improved stiffness and offers a mass reduction of 22% compared to the cast iron bed, hence it can be used for the manufacture of the CNC lathe bed and other machine tool structures for enhanced performance.

Introduction

In modern days, an increased demand necessitates machine tools to produce components of the required geometric form with an acceptable surface finish at high rates of production. An important function of machine tool structures is to assure geometric configuration of the elements under static, dynamic, and thermal loads. The static and dynamic behaviors of these structures depend on the mechanical properties of the materials used for the construction of machine tool structures. Structural materials of machine tools must possess high elastic modulus, yield strength, wear resistance, toughness, high damping, and low thermal co-efficient of expansion.[1,2] Currently, steel and cast iron (CI) are the conventional materials used in machine tool structures. Steel provides compact structure with reduced mass due to high elastic modulus but is limited by poor damping characteristics. The presence of lamellar graphite in CI gives

[1]Department of Mechanical Engineering, PSG College of Technology, Coimbatore, India
[2]Galaxy Machinery Pvt Ltd, Belgaum, India
[3]PSG Institute of Technology and Applied Research, Coimbatore, India

Corresponding author:
Shanmugam Chinnuraj, Department of Mechanical Engineering, PSG College of Technology, Peelamedu Post, Coimbatore 641004, Tamil Nadu, India.
Email: cshanmech@gmail.com

beneficial material damping characteristics and compressive strength as compared with steel.[3,4] However, high shrinkage rate during solidification and more lead time are the setbacks for the use of CI as structural material in machine tools. Also, deterioration of strength and damping properties of CI may reduce the static stiffness of structures against bending and torsion during prolong usage.[5] Further, the components machined using such structures exhibit dimensional variations because of the excessive vibration during machining at high speeds. The static rigidity of machine tool structures is enhanced using either material with high elastic modulus or by improved form designs, but these may not improve the damping properties to reduce vibration effects.[4] These drawbacks of steel and CI lathe have prompted machine tool manufacturers to focus towards alternate materials. Bulk granite stones are used as structural material in high-precision machine tools, but they cannot be used in high-speed machine tools because of the limited long-term dimensional stability, sensitivity to moisture, and less impact resistance.[6]

Machine tool structures made of ferrocement with steel wire mesh have been found to possess comparable stiffness and higher damping characteristics to CI structures, but it leads to complicated fabrication process.[5] Polymer concrete (PC) structures made of quartz, basalt, pebble, fly ash, etc., as an aggregate system bonded with viscoelastic materials (polyester and epoxy resin) possess damping characteristics improved by four to seven times compared to CI structures.[7–9] However, the mechanical properties of PC are greatly influenced by the type of aggregate, resin system, aggregate size, filler, hardener content, moisture level, curing process, time, etc.[10] In general, 80% to 87% of aggregates and 13% to 20% of resin content in PC gives optimum mechanical properties.[11,12] Since the tensile strength of polymer concrete is relatively lesser than that of conventional materials, PC structures are reinforced with steel and CI. Polymer impregnated concrete carriage improves the damping characteristics of machine tool slide ways at low-frequency ranges of 250–650 Hz[13] and the same may not be suitable for high-speed applications. Hybrid sandwich structures made of carbon epoxy bonded with PC composites reduces the weight of machine tool structures by 30% to 37% with an improved stiffness of 16% compared to that of the existing stainless steel structures;[14] hybrid glass epoxy–PC composite offers light weight structure with an improvement in the damping ratio by 35% compared to the CI structure,[15–17] but the mechanical fastening, adequate adhesive bond between the composites, and cost of fabrication are the challenges that limit the usage of hybrid structures. Nowadays, metallic foams are also used in machine tool structures, because of the low mass density, high geometric moment of inertia, and damping capability.[18] Use of

aluminum-foam/ steel sandwich structures in large machine tools offer higher rigidity and weight reduction compared to steel structures.[19] The use of foam materials is hindered by high production and processing cost and the properties are influenced by process parameters and control of foams.

Use of carbon fiber reinforced polymer (CFRP) composites and glass fiber reinforced polymer (GFRP) composites gives light weight structures, since the specific strength of these composites is at least four to six times that of steel and CI. Reduction in mass and energy consumption to the tune of 60% and 70% respectively can be achieved by using CFRP structure in machine tools.[2] Fiber-reinforced composites are also used as cutting tools in machining, a boring bar made of GFRP can hold up to five times heavier depth of cut than steel boring bar before the onset of chatter.[20] A hybrid CI–GRFP grinding machine column showed 35% improvement in damping compared to the CI column, also a hybrid steel–GFRP grinding machine head stock increases the stiffness and loss factor by 12% and 212%, respectively.[15,21] Though fiber-reinforced polymer composites reduce the inertial effects of structural components, fiber flow, orientation, homogeneity among fibers, matrix-fiber interfacial bond, warpage of laminates due to thermally induced stresses and structural weakness other than fiber orientation are the areas of concern.

Currently, machine tool research is also directed towards nature-inspired bionic design, which aims at improving the load-carrying capacity and directional stiffness of structures. Machine tool structures developed based on biological rib bone skeleton and ginkgo root system have been found to possess improved static stiffness and damping by 6%, with a considerable reduction in mass of 6%.[22,23] The requirement of both high stiffness and damping requirements has led to the use of composite materials to replace steel and CI to fabricate machine tool structures.[4,7] Epoxy granite (EG) is a type of mineral-based polymer composite that consists of crushed stones as aggregates bonded by thermoset-based epoxy resin matrix and has better mechanical characteristics compared to other PC composites.[4,24,25] The EG composite can reduce the weight of structures by 50% and improve the damping characteristics by seven to ten times that of CI structures and is an added advantage for high-speed machine tool structures.[4,26,27] Since the elastic modulus of EG is one-third of that of CI, it demands larger structures with thick wall sections.[4] However, within the available work volume constraints, EG structures can be designed with equal or greater stiffness to that of CI structures based on suitable form design rules, topology arrangements using finite element method (FEM).[12,28–30]

There has been not much published information on enhancing static and dynamic characteristics of

machine tool structures using the EG composite. Hence, in this study, an attempt has been made to replace the CI bed of the CNC lathe with an EG composite bed to improve the performance of the CNC lathe against static and dynamic loading conditions. Initially, a finite element (FE) model of the existing CNC lathe bed was developed and analyzed for static and dynamic behaviors. The results of numerical models were validated through experiments. Based on the validated approach, FE model of the lathe bed made of the EG composite was developed and design iterations were carried out to achieve enhanced static and dynamic performance than or at least equal to that of the original CI bed. Finally, the design configuration, which outperforms the CI bed in both static and dynamic aspects of CNC lathe has been selected and recommended for further analysis and fabrication.
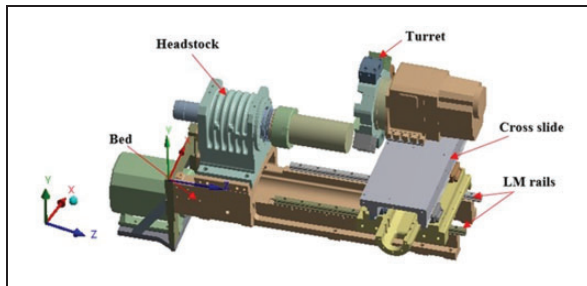

Figure 1. Geometric model of the CNC lathe with principal components.

Static and dynamic analysis of the existing CNC lathe bed

Evaluation of torsional rigidity of the existing CNC lathe bed

The geometric model of the CNC lathe considered for the study is shown in Figure 1. The reaction forces acting on the lathe bed due to cutting forces causes the twisting in addition to bending.

So the lathe bed must be rigid against bending as well as twisting moment. Hence, the torsional rigidity of the existing CI lathe bed was determined using the experiment and a numerical model was developed using FEM. Torsional rigidity of the existing CI lathe bed was experimentally determined using a fixture specially designed and developed as shown in Figure 2(a), The bottom face of the lathe bed was clamped on a fabricated vertical steel frame, which is rigidly fixed on the ground using foundation bolts, and another I beam was rigidly clamped on the top of the lathe bed through which gradually increasing static load was applied using the load cell (Ajay sensors, resolution: 0.1 kg, max load: 1000 kgf). Two linear variable differential transducers (LVDT, Tesa, model: TTD 20, resolution: 0.1 µm, range: ±2 mm) and one-micron dial indicator (1 µm accuracy) were mounted at the bottom of the bed to measure the deflections under each load applied. The coordinate locations of loading and deflection measurement points are shown in Figure 2(b). Load was applied on the I beam at a distance of 767 mm along *X*-axis and 426 mm along *Z*-axis from the head stock
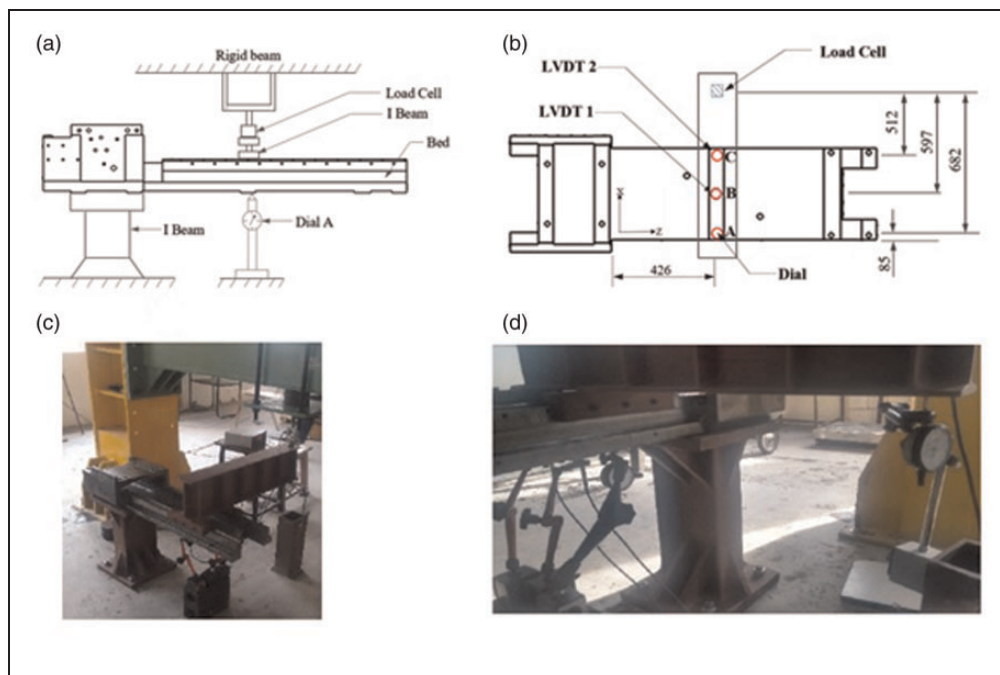

Figure 2. Experimental setup for torsional rigidity test: (a) schematic of the experimental setup; (b) coordinate locations of the load cell and LVDT; (c) CI lathe bed under test; (d) LVDT and dial arrangements.

end as shown in Figure 2(b). The CNC lathe bed used for testing, LVDT and dial arrangements are shown in Figure 2(c) and (d).

Initially, a preload of 20 kg was applied and the LVDT and dial measurements were set to zero, then loads were applied from 0 to 80 kg with an increment of 5 kg and the corresponding deflections at the specified locations were measured. Each test was repeated three times for both loading and unloading conditions and the average values were plotted, using the load versus deflection plot, the fulcrum point was established as shown in Figure 3.

The fulcrum point was established by plotting the distance from loading point against the corresponding deflection at a particular load. The intersection of these plots on the X-axis gives fulcrum point location at 1275 mm and from the same plot, angle of deflection was calculated. Then the torsional rigidity of the CI bed was evaluated as torque per unit angular deflection and was found to be 7.32 Nm/arcsec as listed in Table 1.

Experimental modal analysis on the existing CNC lathe bed

Machine tool vibrations have undesirable effects such as noise, disturbance, and may cause permanent
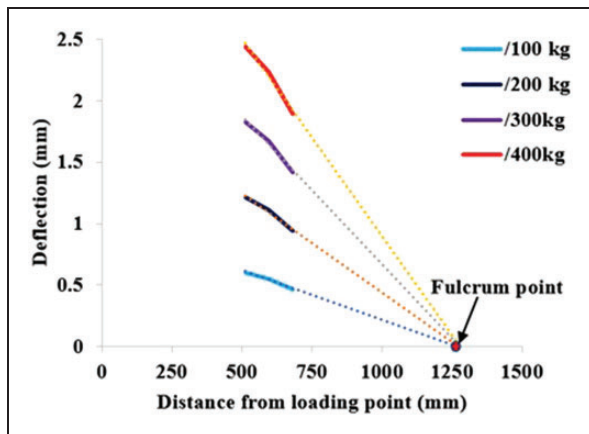

Figure 3. Location of the fulcrum point in load versus deflection plot.

Table 1. Torsional rigidity of the existing CI lathe bed.

Description	Load (kg)			
	100	200	300	400
Torque (load X fulcrum point) (Nm)	1250	2501	3752	5003
Angle of deflection, $\tan^{-1}$ (distance from loading point/deflection) (arc s)	171	342	511	682
Torsional rigidity (Nm/arc s)	7.30	7.31	7.34	7.33

destruction to the structure. Over the decades, there has been a major focus towards a better understanding of the dynamic behavior of structures, identifying the modal parameters namely, natural frequencies, mode shapes, and damping ratios, by machine tool researchers and the field is referred to as modal analysis. These parameters of the bed significantly affect the performance of the CNC lathe and depend on the contact stiffness of butting surfaces, spindle stiffness, position of carriage, turret, and total load on the bed of the CNC lathe. The knowledge on these dynamic parameters is important for the design and manufacture of machine tool structures in order to achieve good surface finish, reproducibility, and chatter-free machining. The experimental modal analysis (EMA) was carried out on the existing CNC CI lathe bed under free–free boundary condition based on the fixed excitation and moving response method using impact hammer with tip made of aluminum (mass: 100 g) and triaxial accelerometer (Bruel & Kjaer, sensitivity: $X = 98.07$ mV/g, $Y = 96.60$ mV/g, $Z = 95.87$ mV/g, temperature: 60–125 °C, surface flatness: 3 μm). The lathe bed was placed on 10 identical springs each of stiffness, $k = 347.8$ N/m as shown in Figure 4, which are designed and manufactured in such a way that the rigid body modes are far apart from the structural modes of the bed.

A total of 33 different locations spread out the lathe bed were selected in order to determine the natural frequency and the corresponding mode shapes as shown in Figure 5. Physical excitation was given along the negative "Y" direction of the bed. Location 11 was selected as the excitation point as it excites both bending and twisting modes of the bed, and was excited using an impact hammer and the response of the bed was measured at different locations using the accelerometer. The responses were stored in the form of acceleration per unit force (g/N) and the natural frequencies were obtained using the frequency response function (FRF) and are shown in Figure 6. The natural frequency, damping ratio, and mode shapes were identified using ME scope software. The first five natural frequencies of the existing CI lathe bed were found to be 283, 315, 682, 736, and 798 Hz, respectively. The fundamental natural frequency of 283 Hz was observed as twisting in the $X–Y$ plane and is characterized by the torsion of LM guides at the turret end. The frequency of 315 Hz is characterized by bending in the $Y–Z$ plane, and at this mode the headstock and LM rails of the bed were subjected to larger amplitude of vibrations. Twisting mode in the $X–Y$ plane was observed for the frequency of 682 Hz and the LM guide was subjected to torsional oscillations similar to the first mode. The fourth natural frequency of 736 Hz was observed as the bending mode in the $Y–Z$ plane, the head stock and the base mounting pad were found to have larger amplitude of vibration due to bending. The fifth natural frequency of 798 Hz was observed as the twisting
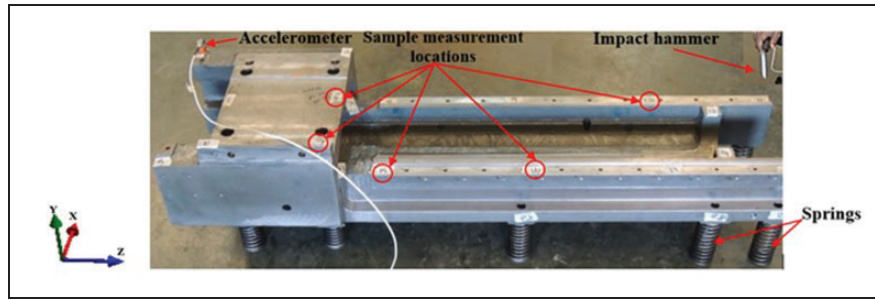
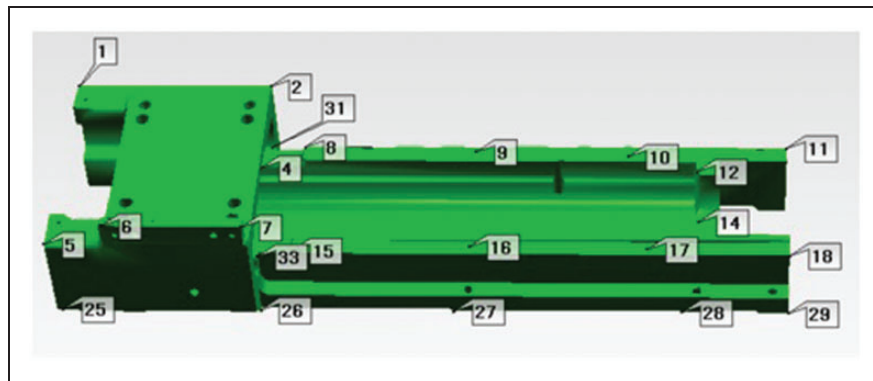**Figure 4.** Cast iron lathe bed on springs for free–free modal analysis.

Figure 5. Geometric model of the cast iron lathe bed with measurement locations.
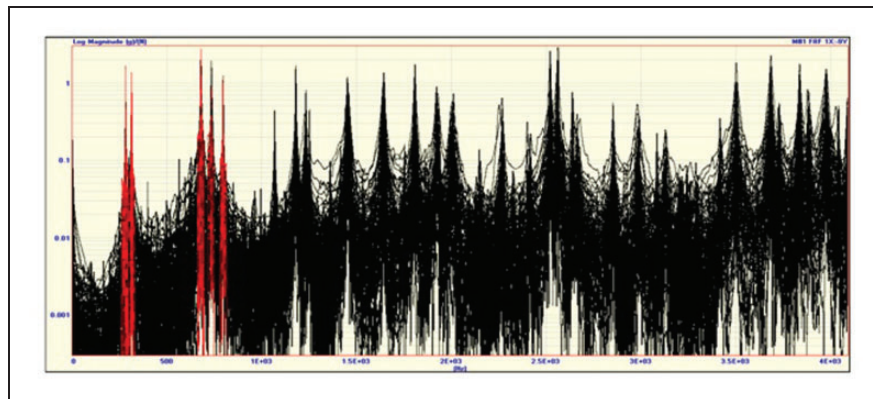

Figure 6. Frequency response functions measured at different locations.

mode in the Y–Z plane and is characterized by twisting of the head stock and the LM guide. The damping ratio was found to be in the range of 0.00043–0.00095 for the identified modes.

Development of the finite element model of the CNC lathe bed

Evaluation of torsional rigidity

In order to build a reliable FE model, initially an FE model of the existing CI lathe bed was developed so as to validate it with experimental results. Geometry of the CI lathe bed was created using CAD modeling software and imported to FEA software in the STEP file format. The material properties of the grey CI were assigned to the FE model of the lathe bed as: Young's modulus $(E) = 110$ GPa, Poisson's ratio $= 0.28$, and density $(\rho) = 7200$ kg/m^3. Static structural analysis of the lathe bed was carried out using hybrid modeling method (HMM) assuming that the rigidity modulus of the supporting and loading beams are several orders higher than that of the bed, so that these elements can be treated as rigid.[31]

The FE model was meshed using higher order hex tetrahedron elements and final mesh size was arrived at through mesh convergence (elements: 34,178,

nodes: 66,640). The bottom surface of the supporting beam was constrained to arrest displacement in "Y" direction, the displacement in "X" and "Z" directions are constrained at four bolt locations and static load
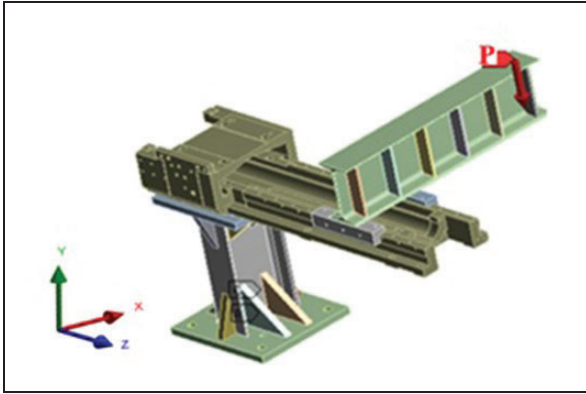

Figure 7. Geometric model of the CI lathe bed for torsional rigidity.

was applied at P ($X = 767$ mm, $Z = 426$ mm from headstock end) as shown in Figure 7. The static structural analysis was carried out to predict the directional deflection of bed at the same locations where the deflections was measured in the torsional rigidity test.

Comparison of the load–deflection plots of the CI bed in the torsional rigidity test at deflections measurement locations A, B, and C is shown in Figure 8. For corresponding to the load of 65 kg, the maximum standard deviation of ± 5.22 µm (300 ± 5.22), ± 5.65 µm (358 ± 5.65), and ± 5.83 µm (391 ± 5.83) was observed in the deflections at measurement locations A, B, and C respectively and are shown in Figure 8 as error bars. Torsional rigidity of the CI bed was calculated using the numerically predicted deflection values as 6.63 Nm/arcsec and is in agreement with the experimental torsional rigidity of 7.32 Nm/arcsec with a maximum deviation of 9%.
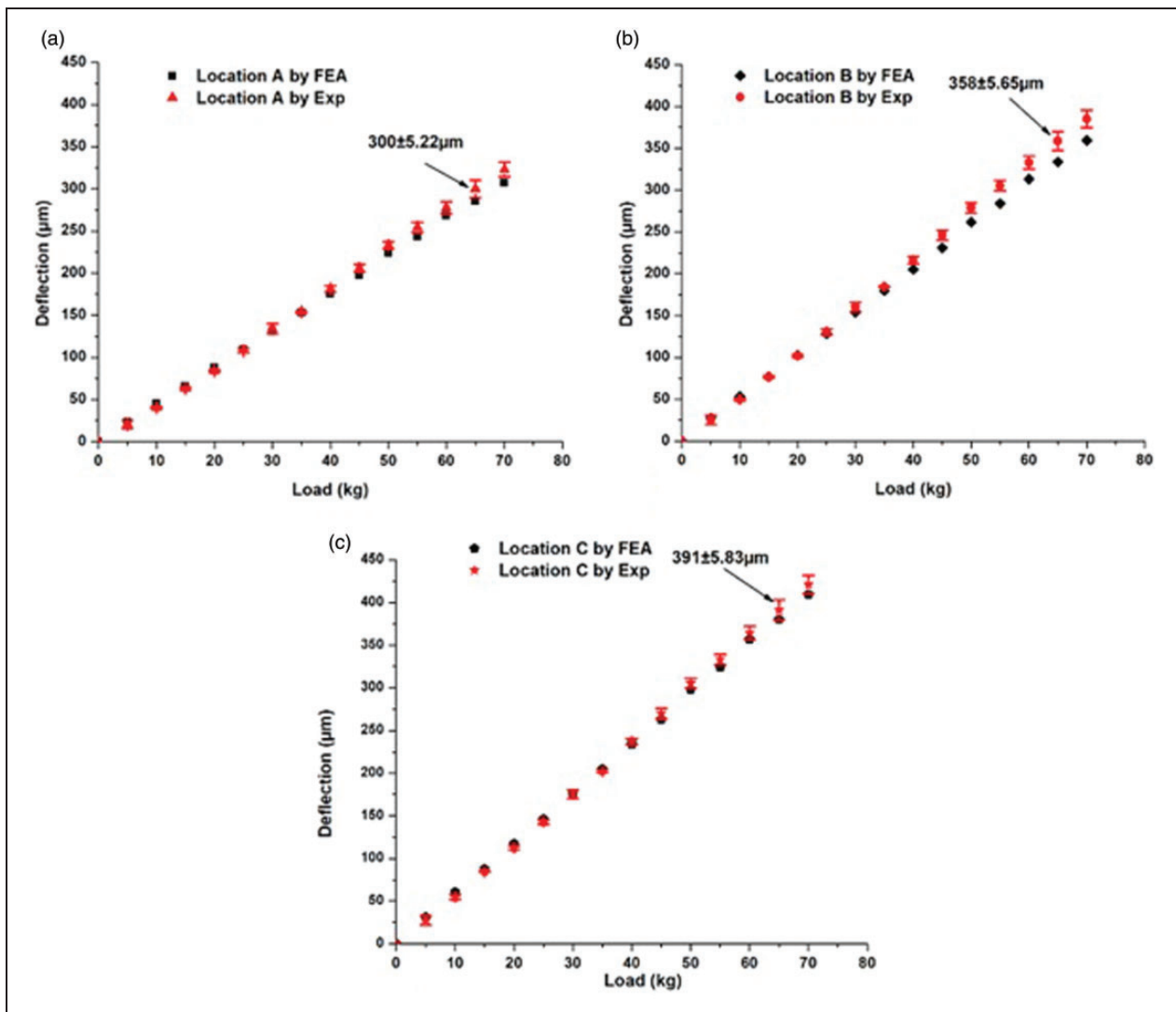

Figure 8. Comparison of load–deflection plots of CI bed in the torsional rigidity test at: (a) measurement location A; (b) measurement location B; (c) measurement location C.

Modal analysis by the finite element method

Modal analysis on the CI lathe bed was carried out under free–free condition using FEA, five fundamental natural frequencies, and corresponding modal parameters were extracted by ignoring the rigid body mode shapes. Table 2 summarizes the results of the experimental and FE modal analysis of the existing CI lathe bed and the mode shapes are compared in Table 3.

It can be seen that there is a good correlation between the numerically predicted and experimentally determined natural frequencies with the deviation of 5% to 9% between them at all identified modes.

Table 2. Natural frequencies of the CI bed.

Mode number	Natural frequency (Hz)			Damping ratio (by experiment)
	By expt.	By FEA	% deviation	
1	283	258	8.8	0.00051
2	315	298	5.3	0.00043
3	682	635	6.8	0.00086
4	736	688	6.5	0.00095
5	798	749	6.1	0.00061
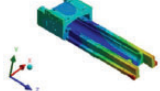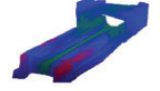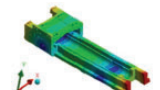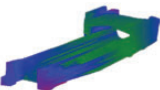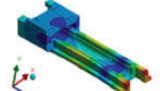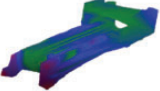
FEA: finite element analysis.

Mahendrakumar et al.[29] adopted the same method to extract the dynamic characteristics of micro lathe bed with the deviation between the experimental and numerical natural frequencies of 3.4% to 9.4%. Hence, the validated FE model can be used for further numerical analysis to study the static and dynamic characteristics of lathe bed structure.

Static analysis of the existing lathe bed by finite element method

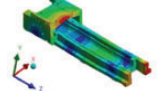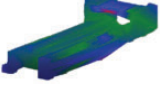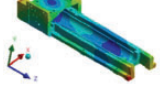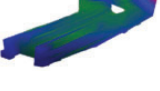The geometric model of the CNC lathe considered for the study is shown in Figure 1. For static structural analysis, in addition to the cutting forces at worst case condition (work piece: SCM 440, insert: MC 6025, power at spindle: 5.5 kW, cutting speed: 200 m/min, depth of cut: 2 mm, feed: 0.25 mm/rev, approach angle: 80°, flank wear: 0.3), weight of important sub-assemblies mounted on the bed, such as head stock (100 kg), carriage and turret (202 kg), motor and motor mounting bracket (65 kg) were considered as shown in Figure 9(a). Worst case cutting force is calculated in order to predict the static deformation developed in the lathe bed. The cutting force components developed during the turning operation are tangential force, F_c the major force component of higher magnitude acts tangential to the direction of the

Table 3. Description of mode shapes of the CI bed.

| Mode number	Mode shape description	Mode shape	
		By FEA	By experiment
1	Twisting in the X–Y plane, more twisting of LM guides at the motor end		
2	Bending in the Y–Z plane, larger amplitude of vibration in the headstock and the motor end of the LM guide		
3	Twisting in the X–Y plane, larger magnitude of twisting of LM guide at the motor end		
4	Bending in Y–Z plane, larger amplitude in the headstock and the base mounting pad		
5	Twisting in the X–Y plane is characterized by larger magnitude of twist of the headstock face and the LM guide		

FEA: finite element analysis.
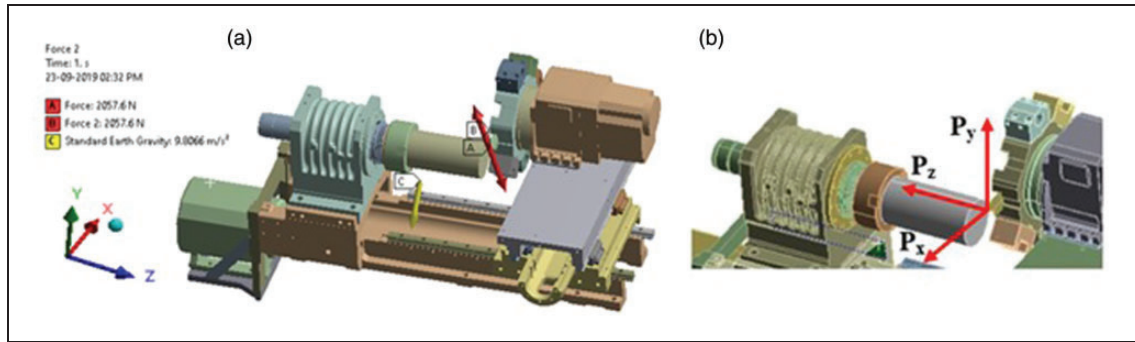
Figure 9. Loading conditions: (a) self-weight and cutting forces; (b) external force.

rotation of the spindle (Y-axis), radial force F_p, acts along X-axis and axial feed force, F_f acts along the Z-axis. The right extreme position of the carriage on the lathe bed along the Z direction and the extreme position of the turret on the cross-rail along the X direction is considered for the static structural analysis of the lathe bed. HMM is used for the static structural analysis and the loading conditions considered for the analysis are shown in Figure 9, and the details are as follows:

1. Self-weight of sub-assemblies without external forces (Case-1)
2. Self-weight of sub-assemblies and worst case cutting forces at the cutting point ($F_C = 1680$ N along Y, $F_f = F_p = 840$ N along Z- and X-axis respectively) (Case-2)
3. Self-weight of sub-assemblies and external force (P) of 1000 N at cutting point each in X, Y, and Z directions, respectively (Case-3)

Two boundary conditions were applied at the interface of bed and base, namely (1) the bed was constrained to arrest displacements in the "Y" direction at six mounting pad locations on the base and bolt locations in the bottom flanges, (2) the displacement in "X" and "Z" directions are constrained at 10 bolt locations as shown in Figure 10.

Initially, the static behavior of the lathe bed due to self-weight of sub-assemblies (Case-1) was analyzed and predicted deformations are listed in Table 4. The headstock was found to deflect more (1.75 µm) owing to the overhung weight of motor mounting bracket assembly under self-weight of sub-assemblies. Under the worst case cutting condition (Case-2), the total deformation of the bed was found to be 2.64 µm as shown in Figure 11, which is twice the deformation of the bed considering the self-weight alone (Case-1) because of the cutting force-induced reaction forces and moments at the bed and head stock interface. Total deformation of the bed at the turret end was found to be less because of more constraints at this end.

In order to predict the directional stiffness of the lathe bed, an external force of 1000 N each in X, Y, Z
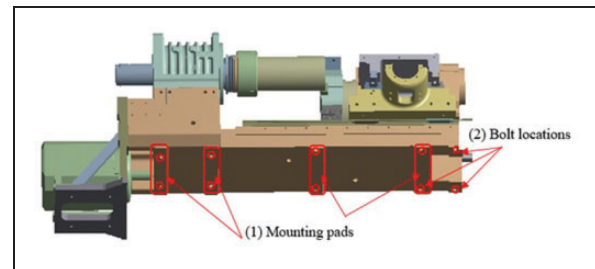

Figure 10. Displacement boundary conditions applied on the lathe bed.

Table 4. Material properties of epoxy granite.[4,33]

S. no.	Properties	Unit	Values
1	Epoxy	Araldite LY 556	
2	Hardener	Aradur HY 951	
3	Granite	Commercially available	
4	Granite aggregate mass fraction	–	0.80
5	Epoxy mass fraction	–	0.20
6	Density	kg/m^3	2300
7	Elastic modulus	GPa	30
8	Poisson's ratio	–	0.25
9	Compressive strength	MPa	110
10	Flexural strength	MPa	36
11	Split tensile strength	MPa	24
12	Damping factor	–	0.0176

directions and the corresponding reaction forces were applied at the cutting point along with self-weight (Case-3) and the predicted deformations are listed in Table 5. As observed from Table 5, the deformation was found to be more at the headstock due to the reaction moment and the twisting effect of the external force. The directional deformation of the bed in the loading direction was found to be more as compared to other directions, except that in the "Y" direction, since the applied external force is opposite to the gravity effect. From the deformation results, the
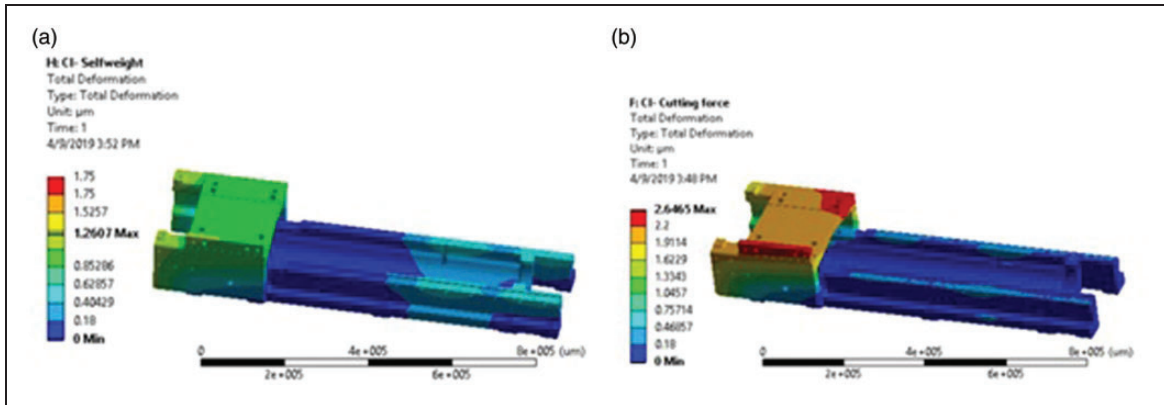
Figure 11. Deformation of the CI lathe bed due to: (a) self-weight; (b) cutting forces.

Table 5. Comparison of deformations of the lathe bed made of CI and EG (Cases 1 and 2).

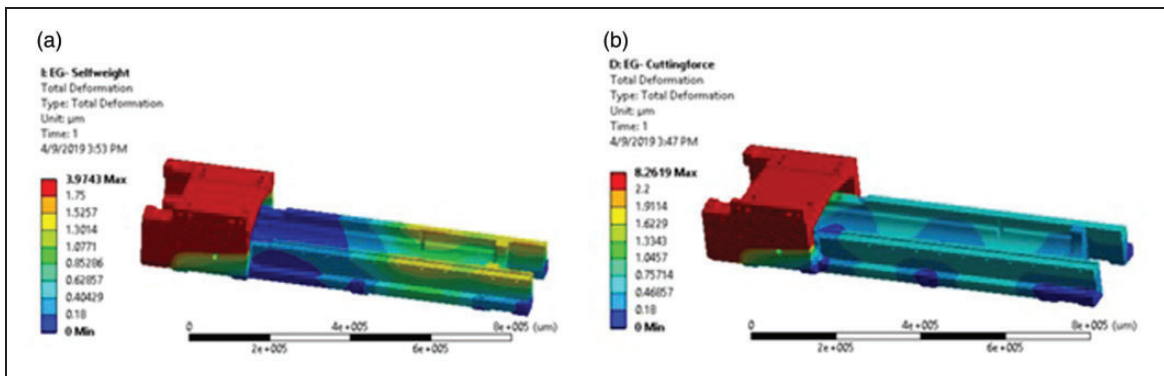| Lathe bed	Loading condition	Directional deformations (μm)			Maximum total deformation (μm)
		X	Y	Z	
Cast iron	Case-1	1.007	0.292	0.714	1.75
	Case-2	2.45	1.13	1.10	2.64
Epoxy granite	Case-1	3.09	0.82	2.29	3.97
	Case-2	7.73	3.31	3.55	8.26

Figure 12. Deformation of the EG lathe bed due to: (a) self-weight; (b) cutting forces.

directional stiffness of the existing CI bed was calculated as 0.65 kN/μm, 33 kN/μm, and 0.980 kN/μm in *X, Y*, and Z directions, respectively.

Design and analysis of the epoxy granite lathe bed

The FE analysis on the existing design of the CNC lathe bed was carried out by replacing CI with EG as the structural material. The material properties used for EG are listed Table 4.

The EG bed was analyzed as per the loading conditions, 1 and 2 (Cases 1 and 2) respectively with the same boundary conditions applied to the CI bed as shown in Figure 10. Table 5 summarizes the deformations in the CNC lathe bed made of CI and EG materials.

The total deformation plot of the EG lathe bed due to self-weight (Case-1) and cutting forces (Case-2) are shown in Figure 12. As observed from the figure, the total deformation of the EG lathe bed at the headstock, due to self-weight and cutting forces, was found to be 3.97 μm and 8.26 μm, respectively. For the same loading and boundary conditions, the EG bed was found to deflect more and is approximately three times that of the deformation of the CI lathe bed, because the elastic modulus of the EG material is one-third that of the CI.

The static structural analysis of the EG bed was performed as per the loading condition 3 (Case-3)

and Table 6 compares the directional deformations of the lathe bed made of CI and EG in specific loading directions.

The directional stiffness of the EG bed was calculated as $0.21\,kN/\mu m$, $3.8\,kN/\mu m$, and $0.27\,kN/\mu m$ in X, Y, and Z directions respectively, which is less than that of the CI bed. Since the elastic modulus of the EG is relatively less, they demand a large structure for the equal stiffness than that of CI.[4] This may affect the location of other critical sub-assemblies in the lathe, also adding to the dimensional constraints, which necessitates redesign of the lathe bed configuration so as to achieve stiffness of the EG bed more than or at least equal to that of the existing CI bed.

Development of reinforcement designs

The stiffness of the EG bed could be achieved as that of the CI bed by resorting to a bulk structure, but this will affect the critical dimensions, mass, and functional requirements of other critical elements to be mounted on the structure and this may not be economically viable. The objective is to improve the dynamic characteristics of the lathe by using EG, but the static stiffness of the EG bed must at least be equal or greater than that of the CI bed for better rigidity. Stiffness of the EG bed can be enhanced by form design modifications, which alone may not be sufficient because EG is relatively poor in tensile strength because of the brittleness compared to CI and structural steel. Reinforcing the EG structure with a material with higher elastic modulus will help achieve the required stiffness and strength. Use of reinforcements in polymer concrete in the form of steel fibers of small diameters will help to improve the static stiffness and damping properties of structures.[4,5,30,32] Therefore, steel was used to reinforce the EG bed to reduce the static deformation. The current study focuses on improving the structural stiffness of the EG bed using steel reinforcements. Five steel reinforcements of the EG bed were designed by retaining the foot prints of the existing CI bed to accommodate all sub-assemblies that are mounted on the bed. Steel mounting pads were added at the headstock, LM rail, and base interfaces to meet the assembly constraints and also to achieve the

geometric dimensional accuracy. Since the bed is subjected to combined bending and twisting due to self-weight and cutting forces, steel fibers were introduced at the bottom of reinforcements to withstand the tensile stress. Steel fiber sizes in reinforcement was arrived at by considering the minimum wall thickness of the bed and the wall thickness is maintained at least six times the size of large granite aggregate, and EG beds with different reinforcement were analyzed under the same boundary and loading conditions as that of the CI bed based on the worst case cutting conditions.

In Design-1, longitudinal and cross-steel fibers of 12 mm diameter with rectangular stirrups have been used at headstock portion to improve the stiffness in the Y direction, while on the LM rail butting surfaces triangular stirrups are used as shown in Figure 13(a).

The total deformation for the EG bed (Design-1) was found to be $5.22\,\mu m$, which is about two times the deformation of the CI bed. Hence, there is a need for the additional reinforcement with ribs to improve the stiffness of the bed, and the same has been considered in Design-2 as shown in Figure 13(b). In this design, the double triangular stirrup configuration at the LM rail portion offers rigidity against load in the Y direction and cross-steel fibers are added for rigidity about the Z-axis. There was a significant reduction in the total deformation ($3.29\,\mu m$) as compared to Design-1, but still it is approximately 1.25 times higher than that in the CI bed and hence further improvement in reinforcement is necessary.

In Design-3 shown in Figure 13(c), structural steel pads were added at headstock and base mounting surfaces to meet assembly requirements and to achieve further reduction in the total deformation. Though this design gives greater reduction in the total deformation ($1.875\,\mu m$) when compared to Design-1, it increases the amount of steel content, which may diminish the damping capacity of the EG bed. Design-4 shown in Figure 13(d) has been arrived at by removing complicated stirrup arrangements in Design-3 by adding headstock mounting pad and guideway plates with machining allowance. The guideway plates are interconnected by "U"-shaped equally spaced eight stirrups made of steel fibers. The size of steel fibers was reduced to 6 mm diameter to minimize the mass of reinforcement so as to enhance the natural frequency and to facilitate better filling of larger size granite aggregates in the mold during the manufacture of the EG bed and the total deformation was found to be $1.33\,\mu m$. Increased steel content, lack of mounting features, and less torsional rigidity necessitates the scope for further refinement in the reinforcement design. Design-5 shown in Figure 13(e) has been arrived by incorporating diagonal stirrups for improved torsional stiffness about the Z-axis. Headstock bushings and pedestal mounting pads have been added to facilitate headstock and base assembly. Also, the simplified reinforcement

Table 6. Comparison of directional deformations of the lathe bed made of CI and EG (Case-3).

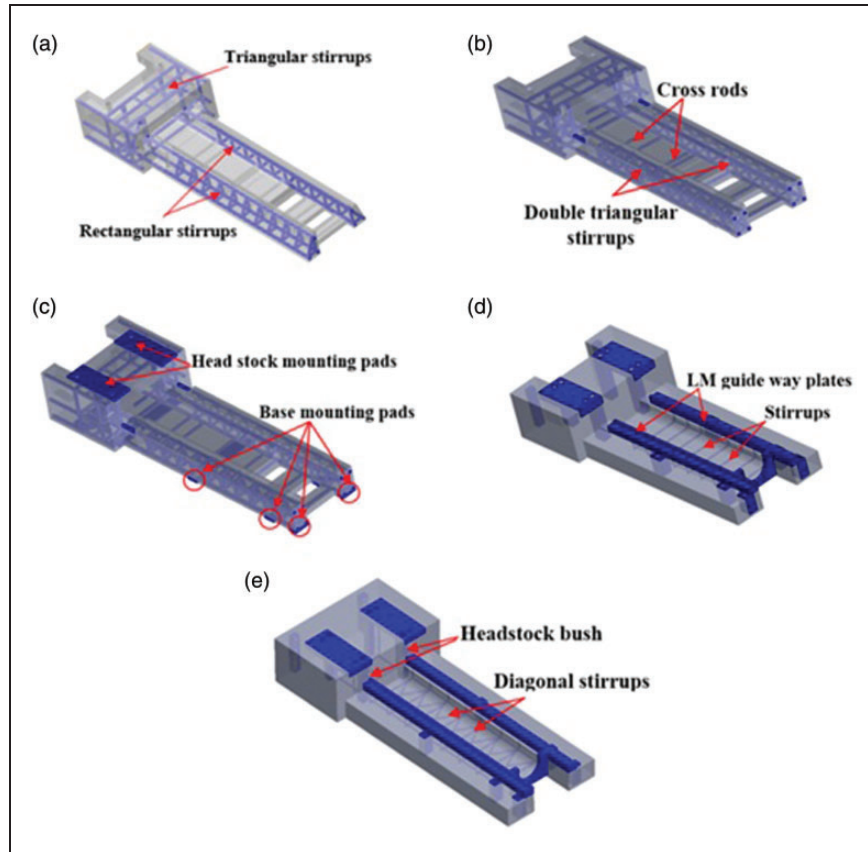| S. no. | Loading direction | Directional deformations (μm) | | | | | |
		Cast iron bed			Epoxy granite bed		
		X	Y	Z	X	Y	Z
1	X-axis	1.53	0.12	0.63	4.63	0.57	2.25
2	Y-axis	0.24	0.03	0.61	0.85	0.26	2.26
3	Z-axis	0.76	0.12	1.02	2.47	0.44	3.61

Figure 13. Steel reinforcement designs of the epoxy granite bed: Design 1; Design 2; Design 3; Design 4; Design 5.
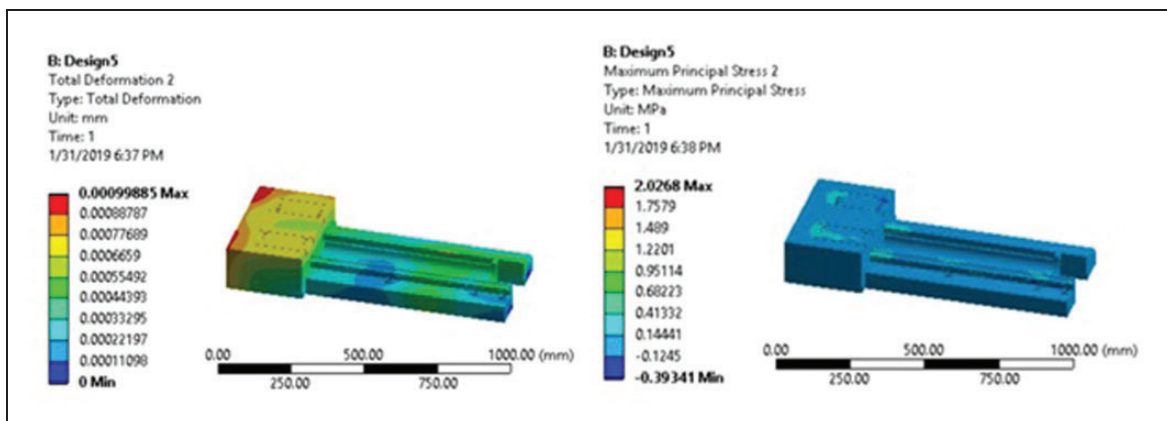

Figure 14. Total deformation and stress plot of Design-5.

design at headstock end ensures the ease of fabrication of the EG bed. It is found that the maximum static deformation of the steel-reinforced epoxy granite (SREG) bed is 0.99 μm as shown in Figure 14, compared to that of 2.64 μm in the existing CI bed under worst case cutting conditions and is about 2.6 times less, which shows the enhanced static stiffness or rigidity of the proposed EG bed. Hence, Design-5 meets the static stiffness requirement and is better than other Deigns 1–4, and the same is proposed as the final steel reinforcement for the EG bed. This steel reinforcement is embedded in the EG bed to achieve

near-net-shape by retaining the core functional features so that sub-assemblies can be mounted over the SREG bed.

The details of five designs and results of static structural analysis under worst case cutting conditions (Case-2) are summarized in Table 7.

The static structural analysis was performed on the proposed SREG bed using the loading condition-3 (Case-3) and the same boundary condition as shown in Figure 10. Table 8 presents the directional deformations in the proposed SREG bed in the specific loading directions.

Table 7. Reinforcement designs of the lathe bed and results of the static structural analysis.

Bed designs	Reinforcement design	Desired effect of reinforcement	Maximum total deformation (μm)	Total mass (kg)	Mass of steel reinforcement	
					(kg)	(%)
Cast iron	–	–	2.64	110	–	–
Epoxy granite	–	–	8.56	32	–	–
Design-1	Rectangular and triangle stirrups, steel fibers of diameter 12 mm	Rectangular stirrups to arrest Y deformation of head-stock, triangular stirrups to arrest Y deformation of LM rails	5.20	52	12	23
Design-2	Double triangle, steel fibers of diameter 12 mm	Stirrups to arrest Y deform-ation of LM rail and cross-steel fibers to resist twisting moment about Z-axis	3.29	56	15	27
Design-3	Double triangle, steel fibers of diameter 12 mm, Integrated with 10 mm plate	Headstock and base mount-ing pads to arrest Y deformation and to meet assembly constraints	1.87	60	20	34
Design-4	Headstock and LM mounting pads with stirrup of steel fibers of diameter 6 mm	Guideway mounting plates to arrest Y deformation of LM rails and stirrups to resist twisting moment about Z-axis	1.33	61	25	41
Design-5	Steel fibers of diameter 6 mm, LM rails interconnected by lateral fibers of 10 nos.	Diagonal stirrups for better torsional rigidity about Z-axis, steel plates with bushes to arrest Y deformation of headstock	0.99	86	19	22

Table 8. Directional deformations of the proposed EG bed, Design-5 (Case-3).

S. No	Loading direction	Directional deformations (μm)		
		X	Y	Z
1	X-axis	0.470	0.524	0.549
2	Y-axis	0.050	0.010	0.546
3	Z-axis	0.080	0.082	0.844

The directional stiffness of the proposed SREG bed is found to be 2.12 kN/μm, 100 kN/μm, and 1.18 kN/μm in *X, Y*, and *Z* directions respectively, compared to the CI bed stiffness of 0.65 kN/μm, 33 kN/μm, and 0.98 kN/μm in the same direction. Chen et al.[30] stu-died the use of artificial granite in machine tool struc-ture, where the results showed the comparable directional stiffness of 36.5 N/μm, 98.4 N/μm, and 130 N/μm in *X, Y*, and *Z* directions to that of the CI structure stiffness of 39.7 N/μm, 111 N/μm, and 125 N/μm in *X, Y*, and *Z* directions but the dynamic characteristics of the artificial granite machine tool structure were improved. The current work shows an improved directional stiffness in the proposed SREG bed with better static rigidity than that of the CI bed.

The proposed SREG bed has to be retrofitted with an existing CNC lathe. The design of the SREG bed is forced to maintain the same foot prints as that of the CI bed, since the sub-assemblies of lathe are the same. Hence, the design iterations of the SREG bed were carried out within the available scope in terms of space constraints, wall thickness, and assembly con-siderations. However, the design can be improved upon through topology optimization using the FE analysis to minimize the steel reinforcement in the EG bed to enhance the dynamic characteristics, which may alter the geometric configuration of the bed. Accordingly, the headstock, LM drive ends are to be designed and developed.

Modal analysis on the proposed epoxy granite bed

In order to study the dynamic behavior of the pro-posed SREG bed (Design-5), modal analysis was performed using FEM under free–free boundary conditions.

Numerically calculated five fundamental natural frequencies and the corresponding mode shapes of the proposed SREG bed are shown in Figure 15. The first fundamental natural frequency of 276 Hz
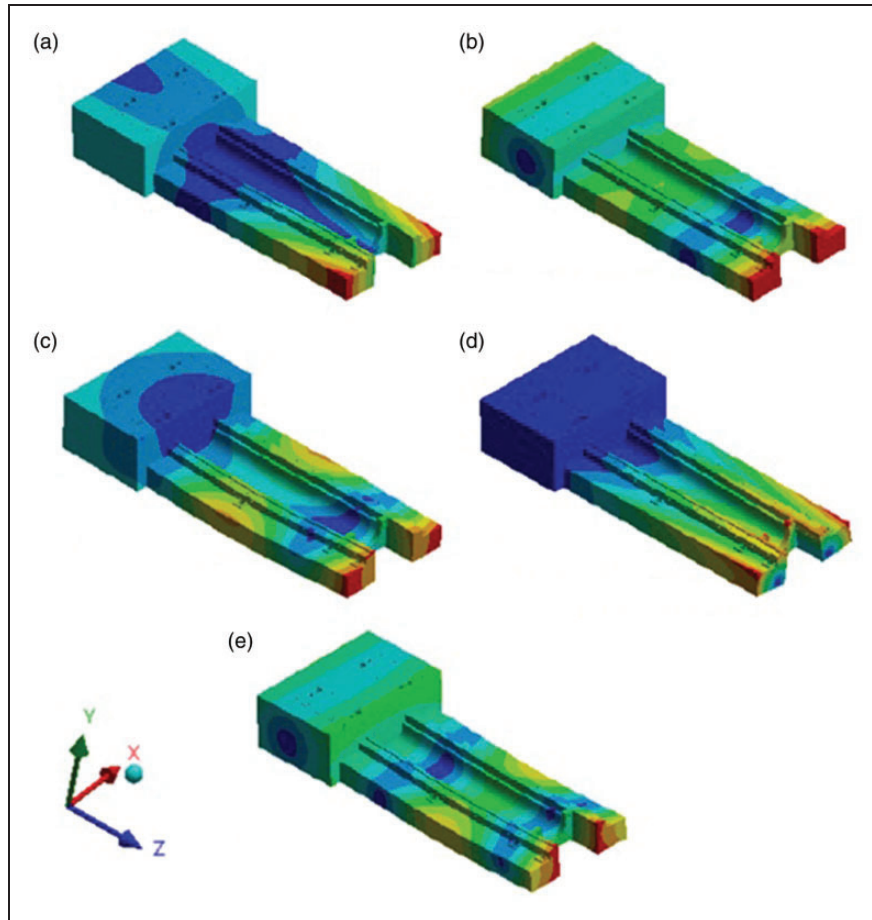
Figure 15. Mode shapes of the proposed steel reinforced EG bed (Design-5): (a) 276 Hz (Twisting in X–Y plane); (b) 336 Hz (Bending in Y–Z plane); (c) 746 Hz (Twisting in X–Y plane); (d) 762 Hz (Twisting in X–Y plane); (e) 854 Hz (Bending in Y–Z plane).

was observed as twisting mode in the X–Y plane. The second mode of 336 Hz as bending in the Y–Z plane, the third mode of 746 Hz as twisting in the X–Y plane, the fourth mode of 762 Hz as twisting in the X–Y plane, and the fifth mode of 854 Hz as bending in the Y–Z plane were observed. Suh and Lee[17] improved the stiffness of machine tool bed with hybrid sandwich structure made of polymer concrete core and welded steel face, also showing an improvement in the damping characteristics of gantry-type high-speed milling machine. Rahman et al.[5,32] presented relatively less static stiffness in the steel fiber reinforced concrete machine tool structure, but the damping ratio was improved three times than that of the CI structure. The results of the modal analysis of the proposed SREG bed show that there is a significant positive shift in natural frequencies of 4–10% compared to that of the CI bed in the observed modes at higher frequencies. This increase in the natural frequency is attributed to improved structural stiffness and 22% reduction in mass of the proposed SREG bed as compared with the CI bed. Hence, the proposed SREG lathe bed would perform favorably better than that of the existing CI bed in both the static and dynamic aspects. Since the proposed bed can be casted to the near-net shape, it eliminates the

secondary machining activities and results in less cost machine tool structure.

Conclusion

In this work, an attempt has been made to improve the dynamic characteristics of the CNC lathe bed using particulate-based polymer composite as an alternate material. EG was used as the structural material in the CNC lathe bed due to high material damping, minimal shrinkage, and ability to be casted to near-net shape with good dimensional accuracy. Numerical studies have been carried out using FEM to investigate the effect of using EG composite as replacement to the CI bed of a CNC lathe to enhance the static and the dynamic characteristics of the CNC lathe. Experimental analysis has been carried out to find the torsional rigidity and mode shapes of the existing CI bed. Numerical simulation on the CI bed was performed using the FE model, and the results of static structural (torsional rigidity) and dynamic analysis (natural frequency) were validated using experimental results with maximum deviation of 9%. Using the validated FE model, the CI bed was analyzed with three different loading conditions and, under worst case cutting condition the maximum deformation of

the bed was found to be 2.64 μm. To enhance the static behavior of the EG bed to achieve the stiffness equivalent to that of the CI bed, steel fibers are used as reinforcement for EG. Five steel reinforcement designs (1–5) for the EG bed are designed considering the stiffness, geometric, manufacturing, and assembly constraints. The SREG beds were designed by retaining the functional foot prints of the existing structural elements, retrofitted in the CNC lathe, and are analyzed using FEM. The proposed Design-5 is found to have better characteristics with improved stiffness, with a significant positive shift in the natural frequencies in the range of 4–10%, which contribute to improved dynamic stiffness of the bed. Also, a considerable mass reduction of 22% was achieved in the SREG bed compared to that of the CI bed. The machine tools made of SREG can be operated at high speeds owing to increased dynamic stability and reduced inertial effect, which will help in chatter-free machining leading to higher productivity and also the product quality can be improved with better surface finish. Hence, the EG composite with steel reinforcement is considered to be a suitable alternative material for the manufacture of machine tool structures.

Novelty of the work

A systematic method was established to design and develop a CNC lathe bed made of EG using FEM to enhance the static and dynamic characteristics. The static stiffness was enhanced by proper reinforcement mass distribution, design of stirrup size arrangement considering the load requirements, manufacturing, and assembly constraints. Since the inherent material damping ratio of EG is four to seven times that of CI, the newly proposed bed offers better dynamic stability to the CNC lathe because of the improved dynamic stiffness and damping characteristics.

Declaration of conflicting interests

The author(s) declared no potential conflicts of interest with respect to the research, authorship, and/or publication of this article.

ORCID iD

Shanmugam Chinnuraj https://orcid.org/0000-0001-7346-0188

References

1. Heisel U and Gringel M. Machine tool design requirements for high-speed machining. *CIRP Ann-Manuf Technol* 1996; 45: 389–392.
2. Möhring H, Brecher C, Abele E, et al. Materials in machine tool structures. *CIRP Ann-Manuf Technol* 2015; 64: 725–748.
3. Abele E, Altintas Y and Brecher C. Machine tool spindle units. *CIRP Ann-Manuf Technol* 2010; 59: 781–802.
4. Rahman M, Mansur Md A and Karim Md B. Non-conventional materials for machine tool structures. *JSME Int J Ser C* 2001; 44: 1–11.
5. Rahman M, Mansur MA, Ambrose WD, et al. Design, fabrication and performance of ferrocement machine tool bed. *Int J Mach Tools Manuf* 1987; 27: 431–442.
6. De Bruin W. Dimensional stability of materials for metrological and structural applications. *Ann CIRP* 1982; 31: 553–560.
7. Orak S. Investigation of vibration damping on polymer concrete with polyester resin. *Cem Concr Res* 2000; 30: 171–174.
8. Kim HS, Park KY and Lee DG. A study on the epoxy resin concrete for the ultra-precision machine tool bed. *J Mater Process Technol* 1995; 48: 649–655.
9. Cortes F and Castillo G. Comparison between the dynamical properties of polymer concrete and grey cast iron for machine tool applications. *Mater Des* 2007; 28: 1461–1466.
10. Haddad H and Kobaisi MA. Influence of moisture content on the thermal and mechanical properties and curing behavior of polymeric matrix and polymer concrete composite. *Mater Des* 2013; 49: 850–856.
11. Jung K, Roh I and Chang S. Evaluation of mechanical properties of polymer concretes for the rapid repair of runways. *Compos Part B: Eng* 2014; 58: 352–360.
12. Haddad H and Kobaisi MA. Optimization of the polymer concrete used for manufacturing bases for precision tool machines. *Compos Part B: Eng* 2012; 43: 3061–3068.
13. Rahman M, Mansur MA, Lee LK, et al. Development of a polymer impregnated concrete damping carriage for linear guide ways for machine tools. *Int J Mach Tools Manuf* 2001; 41: 431–441.
14. Cho S, Kim H and Chang S. The application of polymer composites to the table-top machine tool components for higher stiffness and reduced weight. *Compos Struct* 2011; 93: 492–501.
15. Lee DG, Chang SH and Kim HS. Damping improvement of machine tool columns with polymer matrix fiber composite material. *Compos Struct* 1998; 43: 155–163.
16. Lee DG, Suh JD, Kim HS, et al. Design and manufacture of composite high speed machine tool structures. *Compos Sci Technol* 2004; 64: 1523–1530.
17. Suh JD and Lee DG. Design and manufacture of hybrid polymer concrete bed for high speed CNC milling machine. *Int J Mech Mater Des* 2008; 4: 113–121.
18. Neugebauer R and Hipke T. Machine tools with metal foams. *Adv Eng Mater* 2006; 8: 858–863.
19. Neugebauer R, Lies C, Hohlfeld J, et al. Adhesion in sandwiches with aluminum foam core. *Prod Eng Res Dev* 2007; 1: 271–278.
20. Lee DG. Manufacturing and testing of chatter free boring bars. *Ann CIRP* 1988; 37: 365–368.

21. Chang SH, Kim PJ, Lee DG, et al. Steel-composite hybrid headstock for high-precision grinding machines. *Compos Struct* 2001; 53: 1–8.
22. Liua S, Yea W, Loua P, et al. Bionic design for column of gantry machining center to improve static and dynamic performance. *Shock Vib* 2012; 19: 493–504.
23. Zhao L, Chen W-Y, Ma J-F, et al. Structural bionic design and experimental verification of a machine tool column. *J Bionic Eng Suppl* 2008; 5: 46–52.
24. Schulz H and Nicklau RG. Designing machine tool structures in polymer concrete. *Int J Cem Compos Lightweight Concr* 1982; 5: 203–207.
25. Piratelli-Filho A and Levy-Neto F. Behavior of granite-epoxy composite beams subjected to mechanical vibrations. *Mater Res* 2010; 13: 497–503.
26. Mahendrakumar N, Syathabuthakeer S and Mohanram PV. Study of alternative structural materials for machine tools. In: *Proceedings of fifth international & twenty sixth All India Manufacturing Technology, Design and Research Conference (AIMTDR 2014)*, IIT Guwahati, Assam, India, 12–14 December 2014.
27. Selvakumar A and Mohanram PV. Analysis of alternate composite material for high speed precision machine tool structures. *Int J Eng* 2012; 2: 95–98.
28. Drude N, Meier L, Hoffmann H, et al. Model based strategies for an optimized ribbing design of large forming tools. *Prod Eng— Res Dev* 2009; 3: 435–440.
29. Mahendrakumar N, Thyla PR, Mohanram PV, et al. Study on static and dynamic characteristics of nettle–polyester composite micro lathe bed. *Proc IMechE, Part L: J Materials: Design and Applications* 2016; 233.
30. Chen T-C, Chen Y-J, Hung M-H, et al. Design analysis of machine tool structure with artificial granite material. *Adv Mech Eng* 2016; 8: 1–14.
31. Huang DT-Y and Lee J-J. On obtaining machine tool stiffness by CAE techniques. *Int J Mach Tools Manuf* 2001; 41: 1149–1163.
32. Rahman M, Mansur MA and Zhou F. Design, fabrication and evaluation of a steel fibre reinforced concrete column for grinding machines. *Mater Des* 1995; 16: 206–209.
33. Chinnuraj S, Ramaswamy TP, Venkatachalam MP, et al. Optimization of process parameters of epoxy granite for strength and damping characteristics using TOPSIS method. *J Test Eval* 2020.